

Photoexcitation mechanisms and photofission cross section for Bi by 100–300 MeV quasi-monochromatic photons

C. Guaraldo, V. Lucherini, E. De Sanctis, P. Levi Sandri, E. Polli, and A. R. Reolon
Istituto Nazionale di Fisica Nucleare—Laboratori Nazionali di Frascati, I-00044 Frascati, Italy

S. Lo Nigro, S. Aiello, V. Bellini, V. Emma, C. Milone, and G. S. Pappalardo
*Dipartimento di Fisica, Università di Catania, Istituto Nazionale di Fisica Nucleare,
 Sezione di Catania, I-95129 Catania, Italy*
 (Received 9 February 1987)

The photofission cross section of natural Bi was measured in the energy range 100–300 MeV by means of a quasi-monochromatic photon beam. The nuclear fissility P_f was calculated using the recently measured total photoabsorption cross sections. A discussion on the dependence of fissility from the excitation energy E_x shows that a linear dependence of $\ln P_f$ vs $E_x^{-1/2}$ can hardly be assumed over all the considered energy range. The analysis of the data confirms this consideration and shows an evident saturation effect at high excitation energy. As a consequence, in disagreement with recent interpretations, inferring that the modified quasi-deuteron model is the only efficient mechanism in inducing fission of Bi is less compelling, and also the pion photoproduction excitation mechanism plays a role.

I. INTRODUCTION

The photofission process is a powerful tool for investigating the complex dynamics of heavy nuclei excitation, due to the well-known properties of the electromagnetic interaction and to the large cross section for this process. Particularly interesting is the study of the photofission of elements lighter than uranium at excitation energies well above the giant dipole resonance, where pion production and isobaric excitation become energetically accessible. Moreover, for preactinide nuclei, whose fission thresholds are of the order of 20–30 MeV, fission events from giant dipole resonance photons are practically suppressed.

However, for these nuclei, it is not completely clear which mechanism of photon excitation—by a neutron-proton pair inelastically scattered, or by pion reabsorption—is relevant in producing fission. For these reasons this process was extensively investigated at energies higher than 40 MeV employing principally bremsstrahlung photons.^{1–10} A rapid increase of the photofission cross section, with increasing energy up to 400 MeV, was observed for the first time by Bernardini *et al.*¹ on Bi and was interpreted as due to the onset of pion photoproduction near 140 MeV. The same effect was successively pointed out in other nuclei and was explained in the same way.^{2–5,7} On the contrary, in a work of Moretto *et al.*,⁶ dealing with electron- and photon-induced fission of heavy and medium-heavy elements, the rapid increase in the photofission cross section was accounted for by the increase of the fission probability with increasing energy. Moreover, these authors deduced that the photon interaction described by the quasi-deuteron model is the dominant one in producing fission of lighter nuclei, even at energies well above the pion threshold.

A few years ago, we measured⁹ the Bi photofission cross section between 120 and 275 MeV by using quasi-monochromatic photons from positron in-flight annihilation and suggested that *both* quasi-deuteron and pion photoproduction mechanisms play a major role in producing excitation leading to fission. Subsequently, Arruda-Neto *et al.*¹⁰ studied the electron-induced fission of Bi, in the energy range 43–250 MeV, and determined the photofission cross section by means of the virtual-photon technique. Their results are in substantial agreement with ours. Nevertheless, in contradiction with our conclusions, they deduced, by applying in a questionable way the prediction of the statistical model, that the Lvinger's modified quasi-deuteron photoabsorption mechanism accounts for *all* the compound nucleus formation cross section, through which fission is induced, even above 150 MeV.

These different interpretations of the experiments motivated us in performing a careful study of photofission of Bi, extending our previous measurements⁹ and improving the data analysis procedure, in order to investigate the energy dependence of nuclear fissility over a wider photon energy range. As a matter of fact, unlike the case of uranium, for preactinides, the fissility is a strong function of the excitation energy and, consequently, depends on the photoexcitation process. Therefore its knowledge can give crucial information to disentangle the above controversial interpretations. For this study we took advantage of the characteristics of the Frascati quasi-monochromatic photon beam, which, as it was shown in a previous work,¹¹ offers evident advantages by respect to a bremsstrahlung one in studying fission of nuclei with high fission threshold.

In the present work we report on the fission cross sec-

tion measurements of Bi in the energy range 100–300 MeV. The fission cross section was calculated from the experimental yields solving the Volterra equation by using an improved unfolding method. The nuclear fissility was then deduced by taking advantage of the recently measured total photoabsorption cross sections.¹² In dealing with the energy dependence of fissility, the effective excitation energy following the intranuclear cascade stage was taken into account and properly used. From a discussion on photoexcitation mechanisms and the analysis of the experimental results we deduced that also pion reabsorption is relevant in the nuclear excitation leading to fission in nuclei lighter than uranium.

II. EXPERIMENTAL

A. Photon beam

The measurement was carried out using the LEALE (Laboratorio Esperienze Acceleratore Lineare Elettroni) photon beam produced at Frascati by in-flight positron annihilation on a liquid hydrogen target. A detailed description of this facility was previously given¹³ and therefore only its major features will be summarized here. In Fig. 1 the experimental setup of the end station of the facility is shown. The annihilation photons were obtained by allowing the positron beam (typically 10–20 nA average current, 150 Hz repetition rate, and 4 μ s beam burst width) to impinge upon a 0.0118 radiation lengths thick liquid hydrogen target with 0.012 cm kapton windows. The intensity of the positron beam was continuously monitored by a nonintercepting ferrite toroid *M* set on the beam pipe immediately before the hydrogen target and measured by a Faraday cup placed in the focal plane of the dumping magnet *S*.

In addition to monochromatic annihilation photons, bremsstrahlung is also produced. In order to increase the annihilation-to-bremsstrahlung photon ratio, measurements were carried out collecting photons at an angle of 0.8° – 1° with respect to the positron axis. The photon beam spectrum was measured on-line with the experiment

by a pair-spectrometer¹⁴ PS and the photon flux monitored by a gaussian quantameter. The simultaneous measurement of the beam total energy and spectrum allowed a few percent uncertainty in the determination of the annihilation peak intensity. The used photon flux was typically equal to about 5×10^6 annihilation photons per second.

B. Target assembly and fission fragments detector

The fission fragments were detected by means of the glass-sandwich technique.¹⁵ We used metal targets of natural Bi with a surface area of $(50 \times 50) \text{ mm}^2$ and a thickness of 0.1 mm, sandwiched between two glass plates which covered all the sample surface. We employed a thick target in order to get a sufficient number of fission events in a reasonable irradiation time. However, the sandwich was thin enough to negligibly degrade the photon spectrum. In all measurements the same sample of Bi was irradiated. The collimated photon beam struck the glass sandwich at right angles and had a circular spot ($\phi \sim 4 \text{ cm}$) on the target position. After irradiation, the glass plates were submitted to the procedure of chemical etching and optical-microscope scanning as in our previous experiments.¹⁵ The irradiated surface of both glass plates of each sandwich was entirely scanned, in order to get also information on the forward-backward ratio of the detected fragments. This ratio resulted weakly dependent on the photon energy and values 1.05–1.10 were found in agreement with the results reported in Ref. 16. We also scanned the glass surface not in contact with the target and estimated the background contribution due to spurious events in the glass plates themselves. In this way the effect of radiation damages in the glass plates due to the large irradiation dose was checked.

C. Data collection

The fission fragments yields were measured at 23 different energies in the positron energy range 120–300 MeV. The cross sections per equivalent quantum (shortly called “yields”) were obtained from the numbers of fission tracks counted in the scanned surfaces and the exposure dose measured with the quantameter. We averaged the counts of the two glass plates of each sandwich to obtain results free from a dependence on the forward-backward ratio. The values were obtained in arbitrary units because of the use of a thick target. At three positron energies, specifically 150, 200, and 270 MeV, a thin Bi target was also irradiated. The Bi layer was deposited by thermal evaporation directly on the surface of one of the glass plates. The thickness and the uniformity of the layer were measured by an optical interferometer¹⁷ and through the back-scattering method.¹⁸ The thickness resulted $1.96 \pm 0.05 \text{ mg/cm}^2$. Having taken into account the efficiency of glass plates, as described in Ref. 19, the error in the normalizing factor turned out to be $\pm 7\%$.

III. RESULTS AND ANALYSIS

A. Experimental yields

The experimental yields $g(k_m)$ are connected to the fission cross section $f(k)$ by the Volterra linear equation

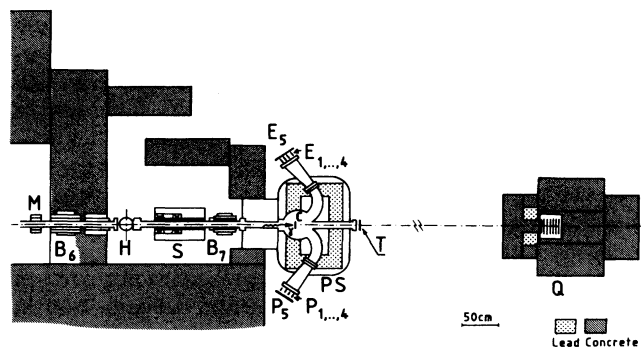


FIG. 1. Layout of the LEALE photon beam end station: B6, magnet; M, ferrite toroid monitor; H, hydrogen target; S, dumping magnet; B7, sweeping magnet; PS, pair spectrometer with the associated electron (E_i) and positron (P_i) detection system; C, photon converter; T, photoreaction target; Q, quantameter.

$$g(k_m) = \int_{k_T}^{k_m} N(k, k_m) f(k) dk, \quad (1)$$

where $N(k, k_m)dk$ is the number of photons in the energy interval $(k, k + dk)$, k_T is the fission threshold energy and k_m is the maximum photon energy.

In Fig. 2 the experimental yields $g(k_m)$ are reported as a function of k_m . The observed oscillations in our points reflect the different experimental situations in each run (photon collection angle, positron and photon beam emittance, etc.). Obviously they do not affect the deduced cross section $f(k)$ values, since the photon spectrum $N(k, k_m)$ was measured on line in each run. In the same figure the relevant experimental data known from the literature,^{1,2,6,7} all obtained by bremsstrahlung photons, are also reported. It appears that our data have a steeper behavior than the results obtained by bremsstrahlung beams. This of course is due to the contribution of annihilation photons in the high energy part of the spectrum.

B. Photofission cross section of Bi

In order to calculate the photofission cross section $f(k)$ from the experimental yields we solved the integral equations (1) by using an unfolding method similar to the numerical one proposed by Cook.²⁰ We improved the accuracy in the representation of the $f(k)$ solution, which was approximated by a natural spline function instead of a stepwise function. In Eq. (1) we have assumed k_m to be equal to the incident positron energy and k_T a suitable energy under which the product $N(k, k_m)f(k)$ is negligible with respect to its average value. We took into account the fission cross section data at energies below 100 MeV (Ref. 8) and we assumed $k_T = 40$ MeV. This could introduce a systematic error in the $f(k)$ solution that we es-

timated to be a few percent at energies $k < 150$ MeV and negligible at higher energies.

The fission cross sections were evaluated for 11 photon energies at intervals of 20 MeV from 100 to 300 MeV. The unfolding method we used, applied to the experimental yields, gave an f vector, which represents an estimate of the photofission cross section averaged in energy by a matrix \mathbf{R} , whose meaning is that of an energy resolution function, as shown by Cook.²⁰ The shape of the \mathbf{R} matrix rows and, consequently, the cross section values, depend on the accuracy of the experimental yields, on the kernel $N(k, k_m)$ of Eq. (1), as well as on the value of a smoothing parameter γ , chosen to regularize the $f(k)$ solution. The parameter γ was selected by applying a Bayesian method, suggested by Turchin *et al.*²¹ This method allows to calculate the probability density $P(\gamma | g)$ of obtaining some γ values for a fixed set of experimental g yields. The $P(\gamma | g)$ function has a sufficiently clear-cut maximum for a number of experimental yields larger than 15, as stated in Ref. 21. For our analysis we had 23 experimental points: this ensured a satisfactory estimate of the γ parameter. The obtained $P(\gamma | g)$ probabilities are drawn in Fig. 3 as a function of some γ -parameter values. We ascertained that there is not a significant change in the $f(k)$ results if one changes the γ values in the range 0.02–0.6, in correspondence of which the $P(\gamma | g)$ probability assumes a value which is the 10% of its maximum reached at $\gamma = 0.1$. The rows of the energy resolution \mathbf{R} matrix obtained for the value $\gamma = 0.1$ are plotted in Fig. 4 for some photon energies. As shown, the \mathbf{R} matrix rows actually have the suitable form of an energy resolution function, except for some small physically meaningless undershoots, with the maximum at the correct energy. This result is a clear indication of the advantages in using an annihilation photon beam for photofission measurements of nuclei with high fission threshold.

The photofission cross section values obtained from the

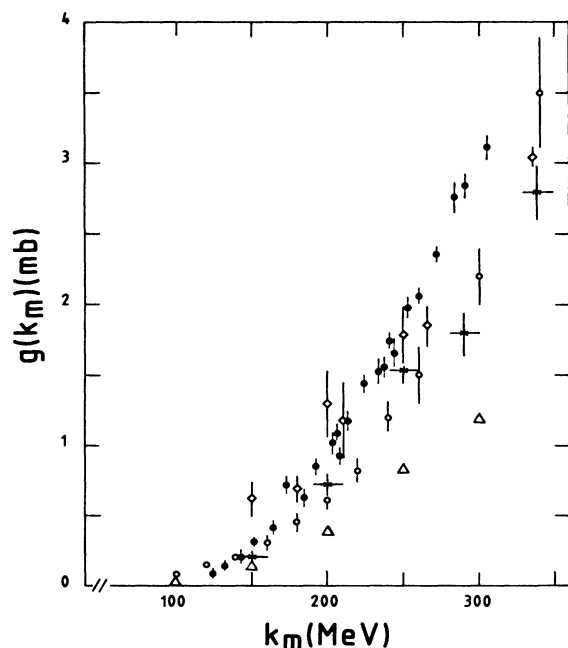


FIG. 2. Photofission yields of natural Bi vs the maximum photon energy k_m . ●, our results; ×, Ref. 1; ◇, Ref. 2; △, Ref. 6; ○, Ref. 7.

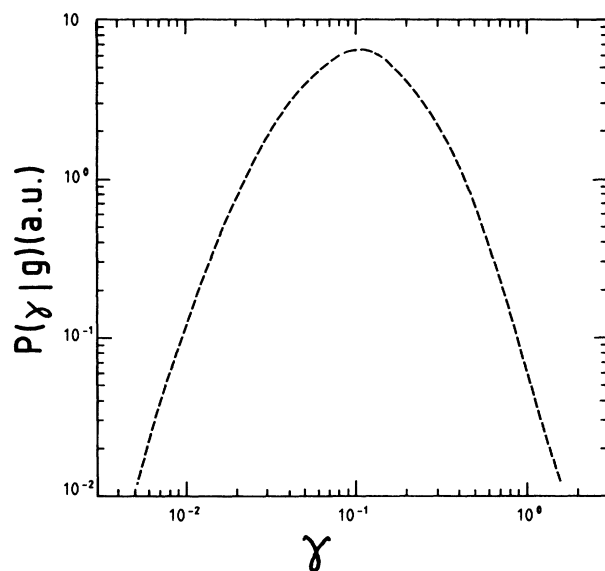


FIG. 3. Probability density $P(\gamma | g)$ as a function of the smoothing parameter γ .

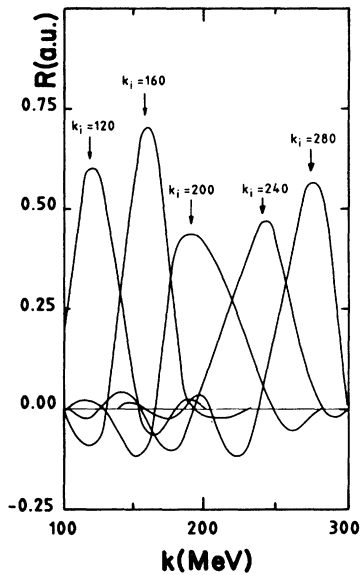


FIG. 4. R matrix rows for $\gamma=0.1$ at different photon energies.

above procedure are reported in Fig. 5. The errors were calculated by the usual propagation rule. They account for the experimental errors as well as for the auxiliary conditions imposed to the solution. The length of the vertical bars of our results actually shows how much the solution is free. In order to take into account the uncertainties in the estimate of the normalizing factors and of the contribution to the fission from photons at energies below 40 MeV a further error equal to 8% should be added. In Fig. 5, all the relevant data concerning Bi deduced in previous experiments^{1-3,6-8,10} are also drawn for comparison. The data of Bernardini *et al.*¹ and Minarik *et al.*³ were obtained by analyzing the experimental yields by means of the photon difference method and with a theoretical bremsstrahlung spectrum. The results of Jungerman *et al.*² (solid curve) were deduced starting from a smoothed curve of the yields and using the photon difference method with a rectangular approximation for the bremsstrahlung spectra. The dashed curve represents the photofission cross sections calculated by Vartapetyan *et al.*⁷ by fitting their experimental yields with an assumed photoabsorption cross section and a constant fissility equal to 0.12. The data of Moretto *et al.*⁶ were obtained by unfolding their electron-induced fission cross section using a theoretical expression to represent the virtual-photon spectra and a suitable numerical method to solve the integral equation of the process. The dot-dashed curve represents the recent data of Arruda-Neto *et al.*,¹⁰ obtained by applying an improved version of the unfolding and virtual-photon technique in the distorted-wave Born approximation to electrofission measurements. The low energy data of Lemke *et al.*⁸ were obtained by using the quasi-monoenergetic photon beam facility of Mainz: they are the only ones—together with the present work's results—to have taken advantage of a monochromatic photon beam.

All data show a similar behavior, even if results of

different experiments scatter also of a factor of 2. On the contrary, it is significant that the recent data from this experiment and from the experiment of Arruda-Neto *et al.*¹⁰ exhibit a substantial agreement, in spite of the different techniques used. At this regard, it must be noticed that, however refined the virtual-photon technique is, measurements with monoenergetic photons are, in principle, a more reliable way of obtaining absolute photofission cross section.

C. Nuclear fissility

From the measured photofission cross section $f(k)$, it is possible to calculate the nuclear fissility P_f defined as:

$$P_f = \frac{f(k)}{\sigma_T(k)}, \quad (2)$$

where $\sigma_T(k)$ is the total photoabsorption cross section. In

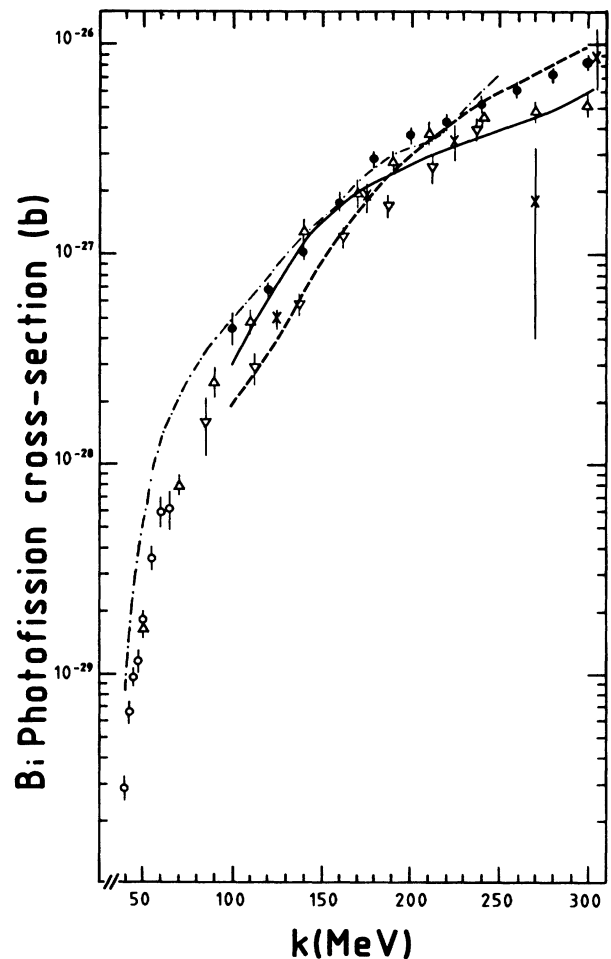


FIG. 5. Photofission cross-section of Bi vs photon energy. ●, our results obtained for $\gamma=0.1$; ×, Ref. 1; ▽, Ref. 3; △, Ref. 6; ○, Ref. 8. The solid curve represents the data of Ref. 2; the dashed curve is the cross section assumed in Ref. 7; the dot-dashed curve represents the results of Ref. 10. As far as the errors on Ref. 10 results, they are not quoted since not deducible from the original paper.

our case, it must be considered that the obtained photofission cross section values were averaged in energy by the matrix \mathbf{R} . Consequently the nuclear fissility was calculated as follows: $\mathbf{R}P_f\sigma_T = \mathbf{f}$, where the product $P_f\sigma_T$ was also averaged by means of the \mathbf{R} matrix.

For $\sigma_T(k)$ we used the experimental results of Carlos *et al.*,¹² who measured the $\sigma_T(k)$ for a different set of heavy nuclei, and whose findings strongly suggest a linear dependence with A of $\sigma_T(k)$, ranging from beryllium to uranium. In Fig. 6 are shown the results we obtained for P_f versus k . The error bars take into account all the experimental errors. In the same figure are also plotted the P_f values deduced from the Lemke *et al.*⁸ $f(k)$ measurements by using the $\sigma_T(k)$ values of Leprêtre *et al.*²² In the figure are also reported the fission probabilities calculated by Moretto *et al.*⁶ and by Arruda-Neto *et al.*¹⁰ by considering the quasi-deuteron mechanism to represent the part of the total photoabsorption cross section leading to compound nucleus formation followed by fission. Their different values over all the energy range are to be ascribed, besides to the different $f(k)$ values, to the different quasi-deuteron models adopted.

As far as the comparison between the present experi-

ment and that of Arruda-Neto *et al.*¹⁰ is concerned, it is clear that—owing to the already found agreement between the photofission cross sections up to 150 MeV (i.e., under the photopion threshold)—the fissility values do also agree, since in this energy range the total photoabsorption cross section is mainly due to the quasi-deuteron mechanism. Above the pion threshold, the different ways of calculating the fission probability lead to diverging P_f values, with an evident saturation effect in our case. The reasons why it is correct to calculate P_f with the full photoabsorption cross section and the physical implications on the photoexcitation mechanisms are discussed in the next section.

IV. DISCUSSION

A. Fission cross section

It is known that, for not too high excitation energies, i.e., according to Table VII-1 of Ref. 23, for energies lower than 50–80 MeV, the fission probability P_f , i.e., the ratio of the fission cross section σ_f to the reaction cross section σ_R , can be approximated by the ratio of the fission width Γ_f to the neutron width Γ_n :

$$P_f = \frac{\sigma_f}{\sigma_R} \cong \frac{\Gamma_f}{\Gamma_f + \Gamma_n} \cong \frac{\Gamma_f}{\Gamma_n} \quad (3)$$

since $\Gamma_f/\Gamma_n \ll 1$. This approximation holds, in particular, for medium-heavy nuclei, such as Bi, which have fission barriers B_f much larger than neutron binding energies B_n (typically $B_f = 20$ – 30 MeV, $B_n \cong 6$ MeV). For these nuclei, in fact, only a small fraction of the reaction cross section goes into fission and the relative probability for fission compared to neutron emission is a strongly increasing function of the excitation energy E_x , so that the so called “second-chance” fission (fission after the emission of the n th neutron) can be neglected. Also, charged particle evaporation is small, with respect to neutron emission, because of the influence of the Coulomb barrier at high Z values.

At higher excitation energies ($E_x \geq 80$ MeV), the ratio Γ_f/Γ_n increases more slowly with energy, the contribution from “second chance” fission becomes significant, and charged particles emission begins to compete so that, according to Ref. 23(a), the approximation (3) is no longer valid, since the ratio σ_f/σ_R is sufficiently large ($\geq 10^{-2}$) that it cannot be reproduced by the values of the ratio Γ_f/Γ_n .

B. Energy dependence of fission probability

The following “high energy limit” can be obtained from statistical considerations for the Γ_f/Γ_n ratio under the assumptions $E_x \gg B_f$, $E_x \gg B_n$:²⁴

$$\ln \frac{\Gamma_f}{\Gamma_n} = C - DE_x^{-1/2}, \quad (4)$$

where C is a quantity varying slowly with energy, $D = a^{1/2}(B_f - B_n)$, $a = a_f = a_n$: level density parameters at the fission saddle point and for the residual nucleus after neutron evaporation, respectively.

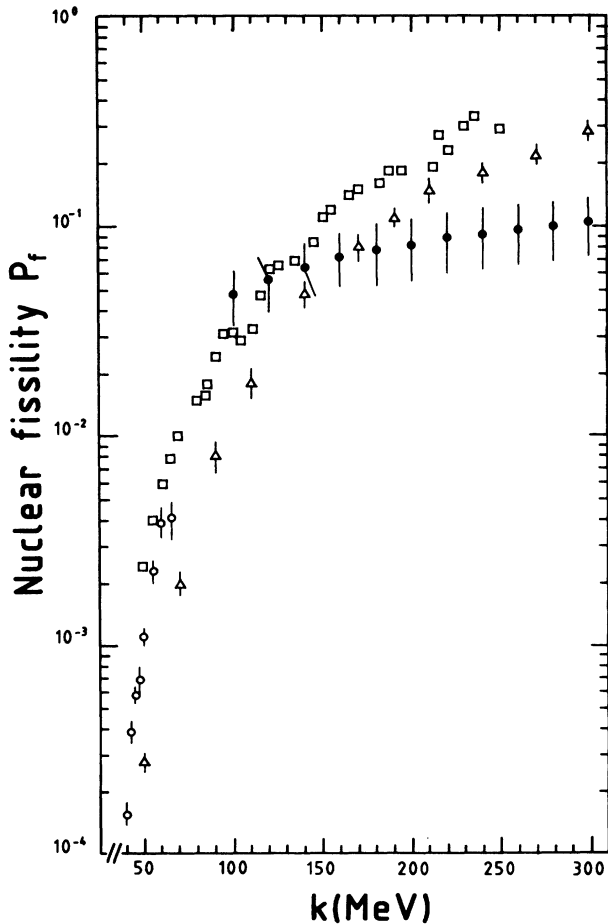


FIG. 6. Fissility vs photon energy k . ●, our results; △, Ref. 6; ○, Ref. 8; □, Ref. 10. As far as the errors on Ref. 10 results, they are not quoted since not deducible from the original paper.

On the full validity of this expression some considerations have to be made. The high energy behavior of Γ_f/Γ_n is not yet entirely understood. If expression (4) does hold, for nuclei such as uranium, for which $B_f \approx B_n$, little excitation energy dependence should be expected. In fact, spallation cross sections for reactions induced by protons with energy above 300 MeV, were reproduced fairly well by treating the initial stages of the reaction by Monte Carlo techniques with the assumption of a constant value for Γ_f/Γ_n , while calculations in which Γ_f/Γ_n was allowed to vary according to Eq. (4) were less successful.^{23(b)}

Another way to check the validity of (4) is the determination of the relative numbers of prefission and postfission neutrons from the angular correlation of the neutrons with respect to the fragment direction, which are, respectively, essentially isotropic and strongly correlated with the fragment direction. In an ^{238}U fission experiment induced by 155 MeV protons the ratio of the above figures was found qualitatively consistent with the energy dependence given by Eq. (4).²⁵ However, additional background processes appear, such as emission of binary fragments, whose kinematic characteristics do not correspond to those of fission fragments and whose cross section can be appreciably larger than fission cross section.

In spite of the seemingly still open problem of the energy behavior of the Γ_f/Γ_n ratio at higher excitation energy, Moretto *et al.*⁶ and, subsequently, Arruda-Neto *et al.*¹⁰ assumed that fission probability retains at high energy the same energy dependence of Γ_f/Γ_n , as given by Eq. (4):

$$\ln P_f = C' - D'E_x^{-1/2}, \quad (5)$$

where C' is a quantity varying very slowly with the energy, $D' = \langle a \rangle^{1/2} (\langle B_f \rangle - \langle B_n \rangle)$ and $\langle a \rangle$, $\langle B_f \rangle$, $\langle B_n \rangle$ are expected to be some kind of averages of the respective quantities a , B_f , B_n for the nuclei along the evaporation chain.

C. Photoexcitation mechanisms leading to fission

According to Moretto *et al.*,⁶ a straightforward consequence of the linearity of $\ln P_f$ versus $E_x^{-1/2}$ was that the photoabsorption cross section predicted by the quasi-deuteron model can account for all the interactions leading to fission in elements lighter than uranium, even at energies well above the pion threshold. Recently, Arruda-Neto *et al.*,¹⁰ assuming both that the Levinger's modified quasi-deuteron mechanism²⁶ (MQD) is effective for compound nucleus formation up to 250 MeV and that almost all the photon energy is converted into nuclear excitation ($k = E_x$), found that the "MQD fission probability" defined as $P_f^{\text{MQD}} = \sigma_f / \sigma^{\text{MQD}}$, where σ^{MQD} was the cross section given by a modified version of the quasi-deuteron model, satisfied Eq. (5) up to high energy, strongly suggesting that only the MQD photoabsorption mechanism was efficient in inducing fission of Bi at all energies.

We want to enter into discussion upon this issue by examining separately the three controversial points on which it is based: (i) the supposed linearity of $\ln P_f$ versus

$E_x^{-1/2}$, consequence of an extrapolation of a statistical approach for the nuclear fission; (ii) the use of the MQD cross section, instead of the total photoabsorption cross section, in calculating the fissility; (iii) the equality between excitation energy and photon energy. It must be noticed that only by making *both* the assumptions (ii) and (iii) the above authors could achieve the point (i).

(i) *Linearity of $\ln P_f$ versus $E_x^{-1/2}$.* This statement can be submitted to some experimental verifications. Arruda-Neto *et al.*¹⁰ recalled that the linear behavior of $\ln P_f$ as a function of $E_x^{-1/2}$ was beautifully demonstrated for the first time by Moretto *et al.*⁶ analyzing systematic measurements of ^4He -induced fission. This claiming indeed must be regarded with some caution. The fact that the energy of the experiment did not exceed 120 MeV allowed, in principle, to approximate the fissility with the ratio Γ_f/Γ_n and therefore, according to Eq. (4), to get the linear behavior of $\ln P_f$. However, as shown in Fig. 7, adapted from Fig. 13 of Ref. 6, a careful inspection of those old data might show a different slope already above 60–80 MeV, so that it does not seem that one can extrapolate some further high energy linearity. Moreover, in calculating the fission probability of Fig. 7, Moretto *et al.*⁶ evaluated the effective cross section σ_0 for compound nucleus formation by an optical model calculation. At this regard, Ignatyuk *et al.*²⁷ observed recently that studies carried out on the spectra of scattered charged particles showed that nonequilibrium (noncompound) processes make a rather large contribution σ_{nc} to the optical model cross section σ_{opt} : $\sigma_0 = \sigma_{\text{opt}} - \sigma_{nc}$. Therefore, also the low-energy linearity could be argument of discussion.

(ii) *Total photoabsorption cross section.* As shown by Arruda-Neto *et al.*,¹⁰ above 140 MeV and up to 250

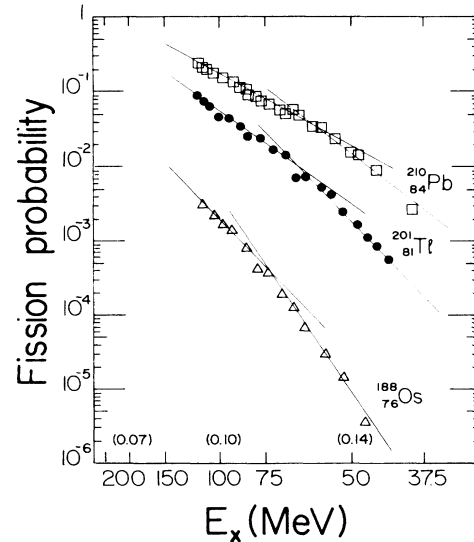


FIG. 7. Fission probability as a function of $E_x^{-1/2}$ for the reactions $^{206}\text{Pb}(^4\text{He}, f)$, \square ; $^{197}\text{Au}(^4\text{He}, f)$, \bullet ; and $^{184}\text{W}(^4\text{He}, f)$, \triangle . Adapted from Fig. 13 of Ref. 6. For convenience the scale of the abscissa gives directly the energy in MeV. In parentheses some values of $E_x^{-1/2}$ are reported. The lines are guides for the eye.

MeV, a straight line for $\ln P_f$ versus $E_x^{-1/2}$ was achieved only if P_f was calculated using the MQD cross section, under the hypothesis that all the photon energy was converted into nuclear excitation energy. On the contrary, the P_f values calculated using the measured photoabsorption cross sections could not be explained in the grounds of the above extrapolation of the statistical model.

Now, above the photopion production threshold, two competing mechanisms play a role in the nuclear photoabsorption: quasi-deuteron and pion production. According to Arruda-Neto *et al.*,¹⁰ the pion reabsorption is ineffective in producing excitation leading to fission of Bi. We now examine this point.

In order to transfer energy, π meson has to be reabsorbed by annihilation on a pair of nucleons (true pion absorption): $\pi NN \rightarrow NN$. Otherwise, pion can be inelastically rescattered before leaving the nucleus or can undergo nonelastic processes such as the Ericson-Ericson-Lorenz-Lorentz effect. In the photon energy range considered 100–300 MeV, the pions are produced with energies between 0 and ~ 150 MeV. The mean free path of a pion in a nucleus has a minimum (~ 1 fm) at the first isobaric resonance, while it is about 7 fm at 40 MeV, and since the nuclear radius of a nucleus such as Bi is ~ 7 fm, the pion can leave the nucleus with a small energy deposition. In this case, however, both the height of the fission barrier and the compound nucleus excitation energy distribution come into play. In fact, a strong influence on the fissility can be exerted by effects due to the change in the properties of highly excited nuclei: calculations carried out with the Thomas-Fermi model and the Hartree-Fock method predict that the height of the fission barrier should decrease appreciably with increasing of the excitation energy.²⁸ Therefore it is reasonable to take into account the pion photoproduction mechanism in producing excitation leading to fission of elements lighter than uranium. As a consequence, in the calculation of P_f , it is straightforward to use the *total* photoabsorption cross section σ_T instead of that given by the MQD model only. As previously said, an accurate knowledge of σ_T was recently made available by measurements¹² which suggested a simple linear dependence of σ_T on A for $9 \leq A \leq 238$. Therefore, it looks just to use these values in the calculation of P_f , destroying the deduction that quasi-deuteron is the only photoabsorption mechanism efficient in inducing the fission of Bi.

(iii) *Equality between photon energy and excitation energy.* It is widely accepted that experimental data on fission of nuclei by particles of intermediate energy are satisfactorily described on the assumption of a two-stage nature of the process.²⁹ In the first, fast stage, the incident particle initiates an intranuclear cascade. As a result, an excited compound nucleus is formed in which, after a certain time, thermodynamic equilibrium is established. Finally, in the second, slow stage, the excited residual nucleus successively evaporates particles or undergoes fission. The produced compound nuclei have a broad distribution in the nucleonic composition, in the angular momentum, and in the value of the excitation energy, the distributions being broader, the higher is the energy of the incident particle. Detailed and systematic Monte Carlo calculations

have been performed for different kinds of inelastic photonuclear reactions for $E_\gamma \leq 1.3$ GeV, in the framework of the intranuclear cascade model.³⁰ This model has made it possible to calculate the different characteristics of photonuclear reactions as a function of the mass number of the target and of the γ -ray energy. In particular, the average excitation energy E_x for nuclei produced following the cascade stage has been evaluated. For photon energy $k \geq 40$ MeV the behavior of E_x versus k is not linear and the average values are both significantly lower than photon energy and smaller for lighter nuclei. In dealing with the dependence of fissility on excitation energy, it seems reasonable to use these predictions instead of the simplified δ -shaped photon energy.

As a consequence of all the complex effects connected with the role played by the excitation energy, one can hardly apply the simple statistical considerations leading to Eq. (5). As a matter of fact, if one plots the results of Arruda-Neto *et al.*¹⁰ with the correct excitation energy, as deduced from the calculation of Barashenkov *et al.*,³⁰ a different slope at higher energy is clearly shown (Fig. 8). In other words, also adopting the same conceptual scheme of Arruda-Neto *et al.*,¹⁰ i.e., by giving the compound nucleus cross section the same magnitude of the MQD cross section, if one uses the correct average excitation energy, again linearity is destroyed.

Then, being useless to follow what appears an arbitrary extrapolation of the statistical model, it is no longer possible any inferring of a specific excitation mechanism. Fig. 9 shows the fissility values versus $E_x^{-1/2}$ deduced from our data (solids dots), together with the results of Arruda-Neto *et al.*¹⁰ and of Lemke *et al.*⁸ (open squares and open circles, respectively) calculated with the total experimental cross sections^{12,22} and with the excitation ener-

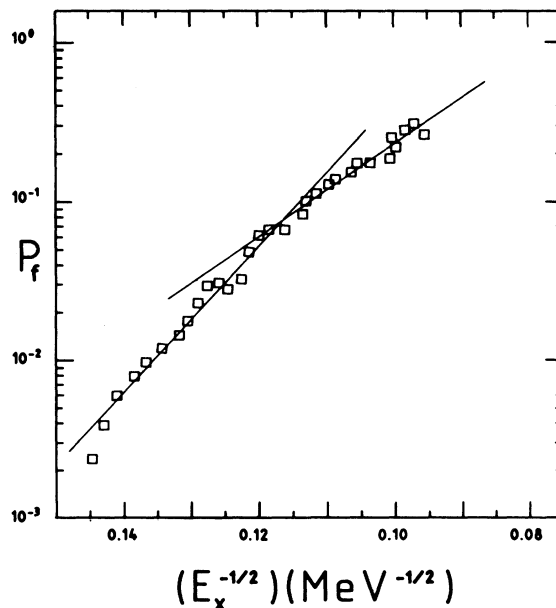


FIG. 8. Fission probability of ^{209}Bi vs $E_x^{-1/2}$. Data from Ref. 10 with the excitation energy deduced from Ref. 30. The lines are guides for the eye.

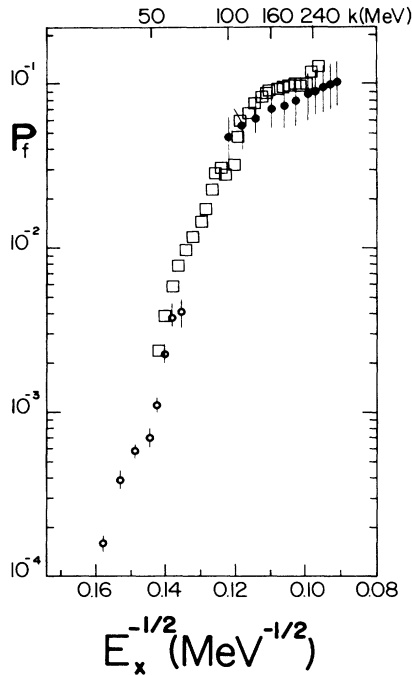


FIG. 9. Fission probability of Bi vs $E_x^{-1/2}$. The excitation energy is deduced from Ref. 30. ●, our results and □, Ref. 10 results with the photoabsorption cross section values from Ref. 12. ○, Ref. 8 results with the photoabsorption cross section of Ref. 22. As far as the errors on Ref. 10 results, they are not quoted since not deducible from the original paper.

gy deduced from Ref. 30. As a consequence of the already found agreement between the photofission cross sections, there is now of course agreement—also above 150 MeV—between our data and those of Arruda-Neto *et al.*¹⁰ As far as the latter are concerned, in the figure the errors are not quoted, since they are not deducible from the original paper. As shown, while it is obviously still impossible to extrapolate a linear dependence of $\ln P_f$ versus $E_x^{-1/2}$ up to 300 MeV, an evident saturation effect is displayed by the fission probability at high excitation energy. This is in agreement with purely probabilistic considerations which predict that fissility must saturate from some energy on. But it is also in agreement with the Glassel *et al.*³¹ consideration that it may become questionable to express the fission probability in terms of the ratio Γ_f/Γ_n , once the statistical model compound nucleus lifetime for neutron (and light particle) emission becomes small compared to the time scale of both the contact time of the prime complex and the dynamical evolution time needed for a fission process—both of the order of several 10^{-21} s—for $E_x > 100$ MeV.

The comparison of our results with the intranuclear cascade calculations allows in particular the investigation of the influence on the fissility of effects such as spread in composition and excitation energy of the residual nucleus, preequilibrium emission, shell effects, uncertainty on the liquid-drop model parameters and dependence of the fission-barrier height B_f on the excitation energy E_x . The cascade model of nuclear reactions and the liquid-drop

model of fission were used by Iljinov *et al.*³² to describe in a unified way the probabilities of fission by different hadronic and electromagnetic probes of intermediate energy (≤ 1 GeV): π , protons, α particles, γ rays. The role of the most relevant effects was separately examined.

(a) *Preequilibrium emission.* Between the fast and slow stages of the process there can exist an intermediate stage of establishment of statistical equilibrium in the residual nucleus. The emission of preequilibrium particles in this stage will change the excitation energy and nucleonic composition of the initial compound nucleus. The calculations³² showed that, other things being equal, allowance for preequilibrium emission will influence greatly the fissility in the sense of a substantial reduction. The effect is enhanced for weakly fissile nuclei ($A \leq 150$) which undergo fission in the first steps of the evaporative cascade where the compound nucleus has a high excitation energy.

(b) *Shell effects.* At high excitation energy (hundreds of MeV) the influence of shell effects is greatly attenuated both by the high value of the excitation energy and by the large spread of the nucleonic composition.

(c) *Uncertainty in the parameters of the liquid-drop model.* In the region of medium nuclei ($A \approx 100$) the fission barrier height is determined mainly by its liquid-drop components. The effect is less relevant for higher masses. According to Iljinov *et al.*³² the most widely used liquid-drop parameters give the fission-barrier height maximum values such as to prevent to describe the experimental data on fissility. Therefore preference must be given to those versions of the liquid-drop model which give lower values of B_f , such as the modified liquid-drop model³³ which takes into account the finite range of nuclear forces.

(d) *Dependence of B_f on E_x .* The sensitivity of the fission barriers to “thermal effects” such as the excitation energy was predicted within the framework of the Thomas-Fermi model and the Hartree-Fock method.²⁸ Using the results obtained by the Hartree-Fock method Il-

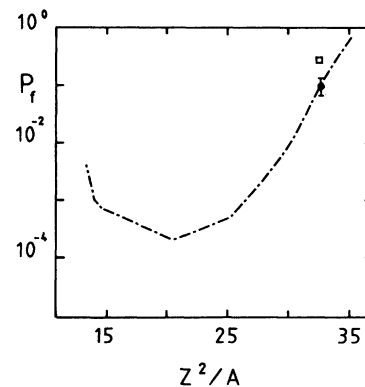


FIG. 10. Fissility behavior vs Z^2/A by 600 MeV photons obtained by the intranuclear cascade calculation of Iljinov *et al.* (Ref. 32) coupled to the modified liquid-drop model of Krappe *et al.* (Ref. 33) (dash-dotted line). ●, our result for 300 MeV photons and □, Ref. 10 result for 250 MeV photons.

jinov *et al.*³² calculated how B_f depends on E_x : for instance, at $E_x \approx 200$ MeV for nuclei with $A \approx 100$, B_f decreases ≈ 15 MeV, while for nuclei with $A \approx 200$ the decrease is ≈ 8 MeV. Of course, the increase of fissility due to the “thermal” decrease of B_f will be strongly compensated when taking into account preequilibrium emission.

In Fig. 10 the fissility behavior versus Z^2/A by 600 MeV photons calculated by an intranuclear cascade Monte Carlo³² coupled to the modified liquid-drop model³³ is shown. Within the accuracy of calculating the mean excitation energy E_x , it was assumed that in the 500–1000 MeV photon energy range the fissility depends weakly on E_x . This is in agreement with the saturation effect displayed by our results at high excitation energies (Fig. 9). The saturation value of fissility obtained from this experiment is reported, as solid circle, in Fig. 10 for comparison. In the same figure the fissility value obtained by Arruda-Neto *et al.*¹⁰ at their maximum photon energy (250 MeV) is also displayed (open square). It is worthwhile to remark the agreement of the intranuclear cascade calculation with our experimental result.

As a matter of fact, at high energy the deexcitation of the nucleus seems to follow channels different from fission, which asks for a new kind of experiment in which not only the photofission cross section, but also the mass and energy distribution of particles and fragments are contextually measured, in particular with lower A targets in which the overall effects are greatly enhanced.

V. SUMMARY OF THE RESULTS AND CONCLUSIONS

Here we summarize our main results and conclusions.

(a) We measured the photofission cross section of natural Bi in the energy range 100–300 MeV by taking advantage of a quasi-monochromatic photon beam (Fig. 5).

(b) The nuclear fissility P_f was calculated using the recently measured total photoabsorption cross sections (Fig. 6).

(c) The energy dependence of fissility was explored by taking into account the average excitation energy E_x calculated in the framework of the intranuclear cascade model (Fig. 9).

(d) The saturation fissility value was compared with the intranuclear cascade calculation result (Fig. 10).

(e) The linear dependence of $\ln P_f$ versus $E_x^{-1/2}$ at high excitation energy (≥ 150 MeV) was demonstrated to represent a questionable extrapolation of a prediction of

the statistical model and a consequence of the use, in calculating the fissility, both of the quasi-deuteron cross section instead of the total photoabsorption cross section, and of an arbitrary identification of the photon energy with the nuclear excitation energy.

(f) It was deduced that, inferring that the quasi-deuteron model is the only efficient mechanism in producing fission, is a less compelling issue if the linearity between $\ln P_f$ versus $E_x^{-1/2}$ does not any longer hold at high excitation energy.

(g) The role played by pion reabsorption as a way to produce nucleus excitation leading to fission was addressed. It was recognized that also this mechanism can come into play, owing to the energy dependence of the height of the fission barrier and to the broad energy distribution of the compound nucleus.

(h) The influence on the fissility of effects such as spread in composition and excitation energy of the residual nucleus, preequilibrium emission, shell effects, variations of parameters of the liquid-drop model, dependence of fission barrier height on excitation energy was explored through a comparison with intranuclear cascade calculations which showed the necessity of taking into account all the above effects and, in particular, displayed the role of the modified liquid-drop model.

(i) As a rather slow process in comparison with particle emission (at least for excitation energies of several tens of MeV) fission can be used as a natural indication of the establishment of statistical equilibrium in the residual nucleus. Therefore in the region of nuclei for which the fission barrier heights are known, from the study of fission it is possible to obtain information on the process of thermalization of the residual nucleus and on the properties of compound nuclei formed. Also, experiments on lighter nuclei, in which not only the total photofission cross section, but also mass and energy distributions of particles and fragments are measured, could possibly elucidate without ambiguity the effective mechanisms of the fission process at high excitation energies.

ACKNOWLEDGMENTS

The authors express their gratitude to M. Albicocco, F. D’Urso, A. Orlandi, W. Pesci, and A. Viticchiè for their continuous technical assistance, to the Linac staff for efficiency in running the machine, and to Mrs. C. Garozzo for the accurate scanning work. This work was supported in part by Centro Siciliano di Fisica Nucleare e Struttura della Materia.

¹G. Bernardini, R. Reitz, and E. Segrè, *Phys. Rev.* **90**, 573 (1953).

²J. A. Jungerman and H. M. Steiner, *Phys. Rev.* **106**, 585 (1957).

³E. V. Minarik and V. A. Novikov, *Zh. Eksp. Teor. Fiz.* **32**, 241 (1957) [*Sov. Phys.—JETP* **5**, 253 (1957)].

⁴Y. N. Ranyuk and P. V. Sorokin, *Yad. Fiz.* **5**, 531 (1966) [*Sov. J. Nucl. Phys.* **5**, 377 (1967)].

⁵A. V. Mitrofanova, Y. N. Ranyuk, and P. V. Sorokin, *Yad. Fiz.* **6**, 703 (1966) [*Sov. J. Nucl. Phys.* **6**, 512 (1968)].

⁶L. G. Moretto, R. C. Gatti, S. G. Thompson, J. T. Routti, J. H. Heisenberg, L. M. Middleman, M. R. Yearian, and R. F. Hofstadter, *Phys. Rev.* **179**, 1176 (1969).

⁷G. A. Vartapetyan, N. A. Demekhina, V. I. Kasilov, Y. N. Ranyuk, P. V. Sorokin, and A. G. Khudaverdyan, *Yad. Fiz.* **14**, 65 (1971) [*Sov. J. Nucl. Phys.* **14**, 37 (1972)].

⁸H. D. Lemke, B. Ziegler, M. Mutterer, J. P. Theobald, and N. Carjan, *Nucl. Phys.* **A342**, 37 (1980).

⁹V. Bellini, V. Emma, S. Lo Nigro, C. Milone, G. S. Pappalardo,

- E. De Sanctis, P. Di Giacomo, C. Guaraldo, V. Lucherini, E. Polli, and A. R. Reolon, *Lett. Nuovo Cimento* **36**, 587 (1983).
- ¹⁰J. D. T. Arruda-Neto, M. Sugawara, T. Tamae, O. Sasaki, H. Ogino, M. Miyase, and K. Abe, *Phys. Rev. C* **31**, 2321 (1985); **34**, 935 (1986).
- ¹¹E. De Sanctis, P. Di Giacomo, S. Gentile, C. Guaraldo, V. Lucherini, E. Polli, A. R. Reolon, V. Bellini, S. Lo Nigro, and G. S. Pappalardo, *Nucl. Instrum. Methods* **203**, 227 (1982).
- ¹²P. Carlos, H. Beil, R. Bergère, J. Fagot, A. Leprêtre, A. De Miniac, and A. Veyssière, *Nucl. Phys.* **A431**, 573 (1984).
- ¹³G. P. Capitani, E. De Sanctis, C. Guaraldo, P. Di Giacomo, V. Lucherini, E. Polli, A. R. Reolon, R. Scrimaglio, M. Anghinolfi, P. Corvisiero, G. Ricco, M. Sanzone, and A. Zucchiatti, *Nucl. Instrum. Methods* **216**, 307 (1983).
- ¹⁴G. P. Capitani, E. De Sanctis, P. Di Giacomo, C. Guaraldo, S. Gentile, V. Lucherini, E. Polli, A. R. Reolon, and R. Scrimaglio, *Nucl. Instrum. Methods* **178**, 61 (1980).
- ¹⁵G. Bologna, V. Bellini, V. Emma, A. S. Figuera, S. Lo Nigro, C. Milone, and G. S. Pappalardo, *Nuovo Cimento A* **35**, 91 (1976); **47**, 529 (1978).
- ¹⁶I. Kroon and B. Forkman, *Nucl. Phys.* **A179**, 141 (1972).
- ¹⁷V. Emma and S. Lo Nigro, *Nucl. Instrum. Methods* **128**, 355 (1975).
- ¹⁸G. Foti, J. W. Mayer, and E. Rimini, in *Ion Beam Handbook for Material Analysis*, edited by J. W. Mayer and E. Rimini (Academic, New York, 1977), Chap. II, p. 21.
- ¹⁹V. Emma, S. Lo Nigro and C. Milone, *Lett. Nuovo Cimento* **2**, 117 (1971).
- ²⁰B. C. Cook, *Nucl. Instrum. Methods* **24**, 256 (1963).
- ²¹V. E. Turchin and L. S. Turovceva, *Sov. Math. Dokl.* **14**, 1430 (1973).
- ²²A. Leprêtre, H. Beil, R. Bergère, P. Carlos, J. Fagot, A. Veyssière, J. Ahrens, P. Axel, and U. Kneissl, *Phys. Lett.* **79B**, 43 (1978).
- ²³(a) R. Vandenbosh and J. R. Huizenga, *Nuclear Fission* (Academic, New York, 1973), p. 217; (b) *ibid.*, p. 239.
- ²⁴J. R. Huizenga, R. Chaudry, and R. Vandenbosh, *Phys. Rev.* **126**, 210 (1962).
- ²⁵E. Cheifetz, Z. Fraenkel, J. Galin, M. Lefort, J. Peterand, and X. Tarrago, *Phys. Rev. C* **2**, 256 (1970).
- ²⁶J. S. Levinger, *Phys. Rev.* **97**, 970 (1955); *Phys. Lett.* **82B**, 181 (1979).
- ²⁷A. V. Ignatyuk, M. G. Itkis, I. A. Kamenev, S. I. Mul'gin, V. N. Okolovich, and G. N. Smirenkin, *Yad. Fiz.* **40**, 625 (1984) [*Sov. J. Nucl. Phys.* **40**, 400 (1984)].
- ²⁸V. S. Barashenkov, A. S. Iljinov, V. D. Toneev, and F. G. Gheregghi, *Nucl. Phys.* **A206**, 131 (1973).
- ²⁹A. S. Iljinov, E. A. Cherapanov, and S. E. Chigrinov, *Z. Phys.* **A 287**, 37 (1978).
- ³⁰V. S. Barashenkov, F. G. Gheregghi, A. S. Iljinov, and V. D. Toneev, *Nucl. Phys.* **A222**, 204 (1974).
- ³¹P. Glassel, D. V. Harrach, H. J. Specht, and L. Grodzins, *Z. Phys.* **A 310**, 189 (1983).
- ³²A. S. Iljinov, E. A. Cherepanov, and S. E. Chigrinov, *Yad. Fiz.* **32**, 322 (1980) [*Sov. J. Nucl. Phys.* **32**, 166 (1980)].
- ³³H. J. Krappe, J. R. Nix, and A. J. Sierk, *Phys. Rev. C* **20**, 992 (1979).